

# Understanding electron-positron momentum densities in paramagnetic chromium

A. Rubaszek

W. Trzebiatowski Institute of Low Temperature and Structure Research, Polish Academy of Sciences,  
P.O.Box 1410, 50-950 Wrocław 2, Poland

Z. Szotek and W. M. Temmerman

Daresbury Laboratory, Daresbury, Warrington, WA4 4AD, Cheshire, United Kingdom

(Received 18 October 2001; revised manuscript received 19 December 2001; published 11 March 2002)

We focus on discrepancies between calculated and three-dimensional reconstructed electron-positron momentum densities in paramagnetic chromium, and consider various effects that can lead to such differences. In this context, the usefulness of the theoretical electron-positron momentum densities for interpreting experimental data, and gaining insight into underlying electronic structure, is also discussed.

DOI: 10.1103/PhysRevB.65.125104

PACS number(s): 78.70.Bj, 71.20.-b

Positron annihilation experimental data provide useful information on the electron momentum density (EMD), and hence, the electronic structure of solids. Two-dimensional angular correlation of annihilation radiation (2D-ACAR) spectra are usually identified with the 2D projections of the three-dimensional (3D) electron-positron ( $e$ - $p$ ) momentum density<sup>1</sup>

$$\rho(\mathbf{p}) = \sum_{\mathbf{k}j}^{occ} \left| \int_{\Omega} e^{-i\mathbf{p}\cdot\mathbf{r}} \psi_{+}(\mathbf{r}) \psi_{\mathbf{k}j}(\mathbf{r}) \sqrt{\gamma_{\mathbf{k}j}(\mathbf{r})} d\mathbf{r} \right|^2, \quad (1)$$

where  $\mathbf{p}$  is the electron momentum in the extended zone scheme,  $\psi_{+}(\mathbf{r})$  and  $\psi_{\mathbf{k}j}(\mathbf{r})$  stand for the positron and electron wave functions (associated with the wave vector  $\mathbf{k}$  and band index  $j$ ), and  $\gamma$  denotes the two-particle  $e$ - $p$  correlation function that, in general, depends on both the electron state  $\mathbf{k}j$  and positron position  $\mathbf{r}$ . Owing to reconstruction techniques, in recent applications,<sup>2-4</sup> these 3D momentum densities could be successfully retrieved from the 2D-ACAR experimental data. The calculated  $e$ - $p$  momentum densities  $\rho(\mathbf{p})$  complement the 3D reconstructed positron annihilation data, providing more insight into the underlying electronic structure of the material under investigation. A direct interpretation of experimental ACAR data in terms of the relevant EMD is, however, very complicated. The same is true for the theoretical  $e$ - $p$  momentum densities. The experimental data are biased by the experimental resolution consisting of the angular resolution of the detector, the thermal resolution as well as smearing caused by the size of the sample vs the size of the positron beam.<sup>1,4</sup> Regarding the reconstruction techniques, all the experimental errors (predominantly the statistical noise) are accumulated during the reconstruction process in the low-momentum region of the 3D spectrum, and appear as oscillations in this region of momentum space,<sup>5,6</sup> while the final resolution function of the 3D spectrum becomes slightly broader as compared to the one of the input 2D-ACAR data.<sup>3</sup> Concerning the shape of the theoretical curves, the results are strongly dependent on details of the band-structure calculations,<sup>7</sup> through the electron wave functions in Eq. (1), the positron distribution as well as the approximation used for the  $e$ - $p$  correlation function  $\gamma$  (for a review see, e.g., Ref. 8).

In the present paper, we discuss a number of possible problems that arise when trying to understand the 3D reconstructed experimental data in terms of the calculated  $e$ - $p$  momentum densities. We base our discussion on the case of paramagnetic chromium for which several 2D-ACAR measurements as well as the 3D reconstructed experimental ACAR data are available.<sup>3,4,9-11</sup> Chromium, a 3d transition metal of bcc structure, is interesting because of its unusual antiferromagnetic state at low temperatures ( $T_N=311$  K), which has motivated positron annihilation experiments both for the paramagnetic and antiferromagnetic phases. Also detailed knowledge on EMD and the underlying Fermi surface of chromium<sup>3,4,9-12</sup> is of great importance for understanding its physical properties. However, as can be seen in Fig. 1, the 3D  $e$ - $p$  momentum densities along the [110] and [111] directions, reconstructed from two different 2D-ACAR data, measured for the paramagnetic phase by two different groups,<sup>3,4</sup> differ substantially from one another in the low-momentum region. This behavior has been observed for the [100] direction as well, but is most pronounced for the [110] direction. An appreciable discrepancy is also seen between these experimental data and the presently calculated  $e$ - $p$  momentum densities, as it was also the case in earlier papers,<sup>9,11,13,14</sup>

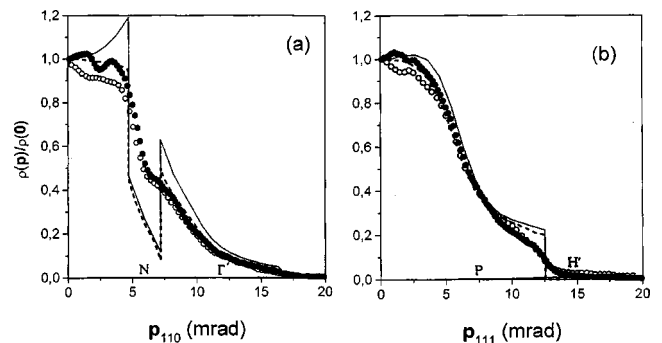


FIG. 1. Electron-positron momentum densities for paramagnetic Cr along the (a) [110] and (b) [111] directions, calculated within WDA (solid line) and IPM (dashed line), compared to the 3D reconstructed experimental results of Refs. 3 (solid circles) and 4 (open circles). All the spectra are normalized to unity at  $\mathbf{p}=0$ . Theoretical curves are not convoluted with experimental resolution function.

especially for momenta close to the  $N$  point along the  $[110]$  direction. The present  $e$ - $p$  momentum densities have been calculated according to Eq. (1) both within the independent particle model (IPM) and weighted density approximation<sup>8</sup> (WDA) for the  $e$ - $p$  correlation function  $\gamma$ . The electron wave functions have been obtained in the local-density approximation (LDA) to density-functional theory,<sup>15</sup> with the Ceperley-Alder exchange-correlation energy functional,<sup>16</sup> using the linear muffin-tin orbitals band-structure method, implemented within the atomic-sphere approximation.<sup>17</sup> The positron wave function has been determined with the same band-structure method, by solving the appropriate Schrödinger equation with a positron potential containing also either the IPM or WDA  $e$ - $p$  correlation potential.

Let us start with establishing how far different measurements can influence information on EMD, and the resulting shape of the Fermi surface (FS), of the studied material. As mentioned above, the two experimental 3D spectra, shown in Fig. 1, differ in their slopes in the low-momentum region. This may be attributed to several reasons such as a different number of measured 2D-ACAR projections used in the 3D reconstruction (four projections used for angles  $0^\circ$ ,  $12^\circ$ ,  $23.7^\circ$ , and  $45^\circ$  vs ten projections measured with constant angle step of  $5^\circ$ , respectively, for Refs. 3 and 4), choice of reconstruction method (Cormack's Ref. 2 vs inverse Fourier transforms), and statistics of the experiment ( $220 \times 10^6$  vs  $8 \times 10^6$  counts per projection, respectively). Also, the temperature at which experiment was performed (about 353 K in Ref. 3, at which the sample can be considered as completely paramagnetic, vs 323 K in Ref. 4, at which residual stains in the sample can sustain the existence of antiferromagnetic phase<sup>9</sup>) plays a role. Regarding the effective resolution (including the thermal resolution) of the 2D-ACAR apparatus, it was very similar for both measurements in question and estimated to be equal to about  $1.5 \times 1.5$  mrad<sup>2</sup> after reconstruction.

Analyzing further the curves plotted in Fig. 1, one can see that the spectrum reconstructed in Ref. 3 shows an unphysical oscillation at about 2.5 mrad. As can be seen especially in Fig. 2(a), this oscillation is strongly enhanced by deconvoluting the experimental data with the resolution function of the ACAR spectrometer. Since, no band-structure calculation that we have performed for chromium (even when taking into account a possible misalignment of the sample) has been able to reproduce this oscillation, we are inclined to conclude that it is either an effect of a statistical error or an artifact of the reconstruction method. For momenta close to the Brillouin-zone (BZ) boundary and higher, the spectra measured by both groups are very similar in their slope. The momentum that corresponds to the position of the full width at half maximum (FWHM) of the experimental curves defines the FS break, and hence, the Fermi momentum in the  $[110]$  direction, and is equal to about 5.2 mrad, for both sets of the experimental data. Note that this value of the Fermi momentum can be much more accurately determined on the basis of the deconvoluted experimental data [see Fig. 2(a)]. The value of the Fermi momentum deduced from the de Haas van Alphen (dHvA) experiment [see Ref. 12] is about 5.04 mrad. However, the Fermi momentum of 4.69 mrad,

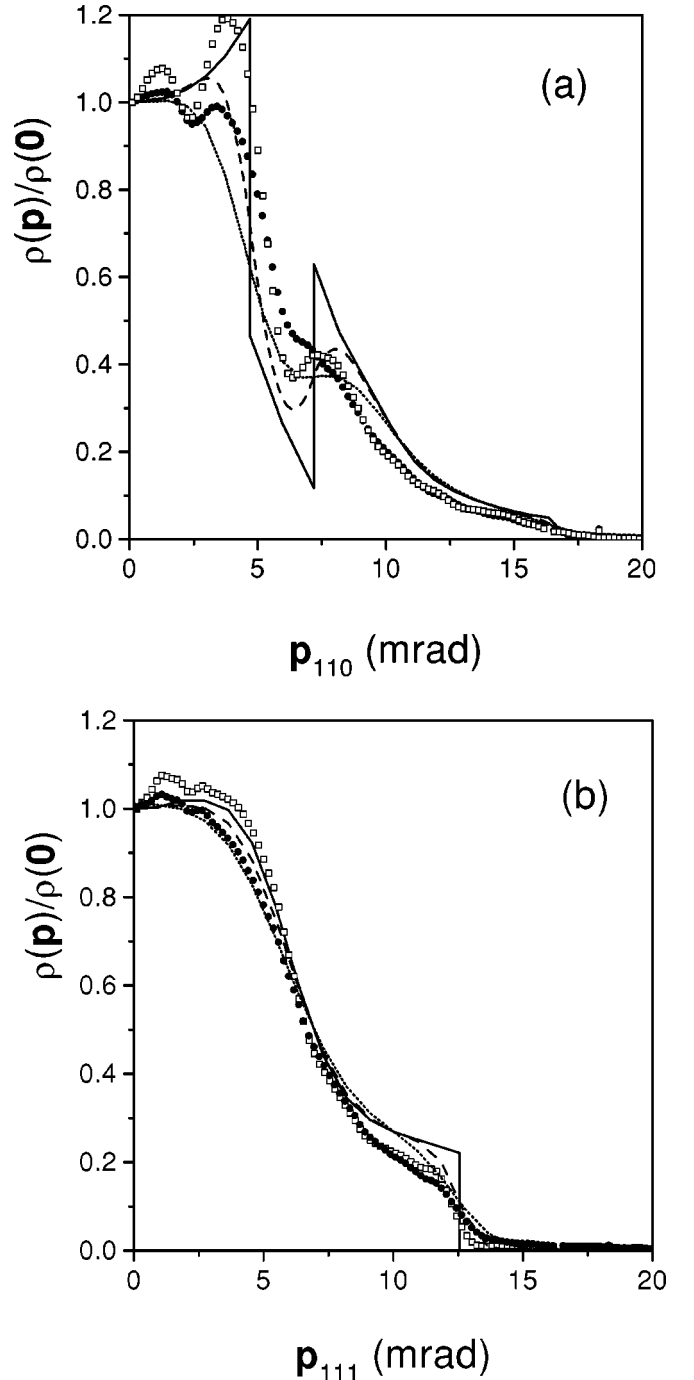


FIG. 2. Electron-positron momentum densities for paramagnetic Cr along the (a)  $[110]$  and (b)  $[111]$  directions, calculated within WDA without convolution with the experimental resolution (solid line), compared to its counterparts obtained through convolution with Gaussians of FWHM equal to 1.5 mrad (dashed line) and 3 mrad (dotted line). Solid circles and open squares refer to the 3D reconstructed experimental spectra of Ref. 3, representing, respectively, the raw and deconvoluted ACAR data.

established on the basis of our calculations [see Figs. 1 and 2(a)] differs noticeably from the values extracted from both the dHvA and ACAR experiments. This difference in the positions of the Fermi surface breaks is especially well seen

when comparing the raw experimental ACAR data with the theoretical curves convoluted with a Gaussian of FWHM=3 mrad [see Fig. 2(a)]: both the experimental and theoretical curves descend almost in parallel towards the  $N$  point. It may be worthwhile to mention here that our calculated value of 4.69 mrad for the Fermi momentum  $k_F$  is in very good agreement with the value of 4.686 mrad obtained from the augmented plane-wave calculation,<sup>14</sup> 4.72 and 4.75 mrad from the full potential linearized augmented plane-wave calculation [for LDA and general gradient approximation (GGA), respectively],<sup>18</sup> as well as, about 4.7 mrad from the pseudopotential method.<sup>4</sup> Note that a very similar discrepancy between the widths of 3D experimental and theoretical momentum densities has also been observed for other bcc metals, namely vanadium<sup>5,8</sup> and tungsten,<sup>4</sup> for momenta along the  $\Gamma$ - $N$  direction. It is interesting that the value of the Fermi momentum, determined on the basis of the experimental spectrum measured at low temperature for the antiferromagnetic phase of Cr, does not differ from the value for the paramagnetic Cr, and both the spectra appear to be very similar in their slopes.<sup>4</sup>

We believe that the difference between the experimental and theoretical “peak-to-valley” ratios, observed both in Cr and V for momenta along the [110] direction, can be explained by the many-body  $e$ - $p$  interaction effects.<sup>9</sup> However, according to the Majumdar’s theorem,<sup>19</sup> the positions of the FS breaks cannot be changed by the  $e$ - $p$  correlation effects (compare the IPM and WDA curves, plotted in Fig. 1). Also, different approximations for the  $e$ - $p$  correlation effects, such as WDA, LDA, and GGA, lead to fairly similar  $e$ - $p$  momentum densities at the Fermi-surface breaks. In Fig. 3, we compare our results for the LDA, WDA, and IPM  $e$ - $p$  momentum densities, and notice that there is very little difference between the LDA and WDA curves, however understandably, they differ substantially from the IPM result, especially when approaching Fermi momentum. Regarding the GGA  $e$ - $p$  momentum density, it follows closely the IPM result.<sup>13</sup> Therefore, one could speculate that the difference between theory and experiment in the value of  $k_F$  and the size of the  $N$  hole, seen in Figs. 1 and 2(a), should be attributed to other correlations, e.g., electron-electron correlations. Of course, the fact that the 3D experimental curves in Cr and V are considerably broader along the [110] direction, and in Cr substantially more isotropic than it would follow from the band-structure calculations, has to be at least partially associated with the reconstruction process, which seems to provide less anisotropic EMD for the bcc metals, especially for open directions like the [110] direction. Since, however, the theoretical results differ also from the dHvA predictions, an inadequate description of electron-electron correlations has to be considered as another possible cause of discrepancy between the experimental and calculated spectra. We shall discuss this in some detail later.

Inspecting carefully the comparison between the calculated curves and experimental data in Fig. 1, one can see that for small values of momentum  $\mathbf{p}$  the calculated momentum densities differ in slope from the experimental spectrum obtained in Ref. 4. Surprisingly, the IPM momentum density seems to reproduce quite well the shape of the experimental

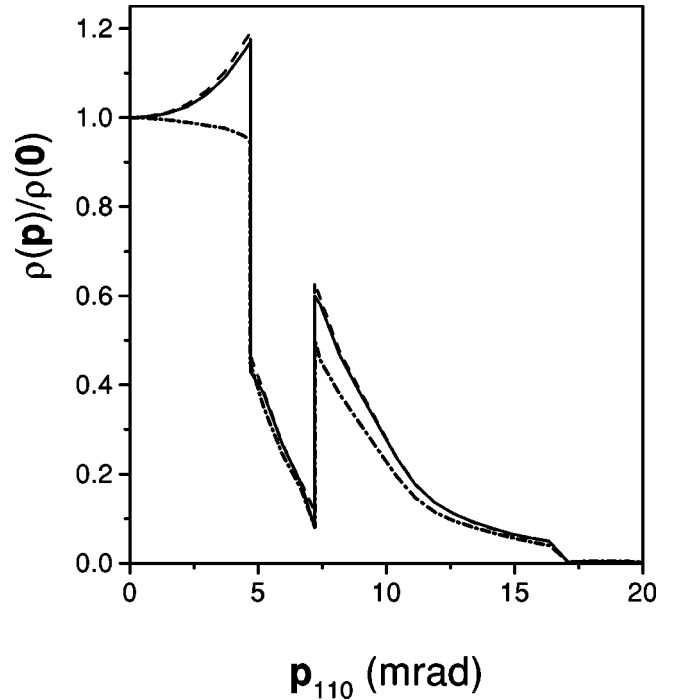


FIG. 3. Electron-positron momentum densities for paramagnetic Cr along the [110] direction, calculated within WDA (solid line), LDA (dashed line), and IPM (dash-dotted line). All curves are normalized to unity at  $\mathbf{p}=0$ .

spectrum of Ref. 3, much better than the physically more realistic WDA result, taking into account the electron-positron correlations. Our WDA calculation for the [111] direction [see Fig. 2(b)] agrees very well with  $\rho(\mathbf{p})$  obtained in the Bloch modified ladder-approximation theory,<sup>14</sup> proving that WDA provides an adequate description of the  $e$ - $p$  correlations in this system. Regarding the width of the spectra along the [111] direction, unlike in the [110] direction, here theory and experiment agree reasonably well. Note, however, that in the first BZ there is no FS break in the [111] direction, while in the [110] direction there is. It seems that for reproducing this kind of discontinuity, associated with bands crossing the Fermi level, the reconstruction techniques may need more projections, especially that the [110] direction is so open.

Figure 2 illustrates the effect of the finite resolution of the ACAR apparatus that can be dealt with in two ways: by deconvoluting experimental data with the resolution function<sup>3</sup> or by convoluting the calculated momentum density with a relevant Gaussian, mimicking the resolution function.<sup>1</sup> In the present work, when convoluting the calculated momentum densities with a 3D Gaussian we have considered two substantially different values for its FWHM: the first equal to the experimental estimate after reconstruction, namely, 1.5 mrad, and the second to be considerably overestimated at 3 mrad. The latter has been chosen to show that, similarly to the experience of Matsumoto and Wakoh,<sup>11</sup> a much larger resolution would be needed to improve agreement with experiment (see Fig. 2). In order to elucidate the effect of the resolution function on the shape of the calcu-

lated and experimental 3D momentum densities, in Fig. 2 we have compared the “pure” (unconvoluted) WDA result with two other curves obtained from the WDA result by convoluting it with Gaussians of, respectively, 1.5 and 3 mrad widths. In this figure we have also presented the deconvoluted and raw 3D-ACAR spectra. There is no doubt that the agreement between theory and experiment is substantially affected by the resolution of the ACAR experiment. The unconvoluted WDA result reproduces very well the shape of the deconvoluted ACAR data for momenta inside the central FS, however, with the exception of the position of the FS break. The agreement between the raw experimental data and the convoluted theory is also quite satisfactory, and improves with increasing the FWHM of a Gaussian, as also found by Matsumoto and Wakoh.<sup>11</sup> That convoluting the theoretical momentum densities with the resolution function smoothes out sharp discontinuities at the FS can be best seen when comparing the “pure” WDA curve with those corresponding to the convoluted curves, respectively, with the FWHM of 1.5 and 3 mrad. Finally it should be noted here that taking into account the effect of the experimental resolution in calculated WDA momentum densities alters the resulting values of  $\rho(\mathbf{p})$ , both qualitatively and quantitatively, similarly to when neglecting the  $e$ - $p$  interaction effects in Eq. (1).

As mentioned above, treatment of electron-electron correlations is another effect that can possibly influence the shape of the calculated  $e$ - $p$  momentum densities. All band-structure methods, providing input to the calculations of  $\rho(\mathbf{p})$ , are based on the density-functional theory<sup>15</sup> that leads to one-electron quantum-mechanical equations whose solutions are only auxiliary quantities providing an approximation to the true quasiparticle spectrum of the full many-body problem. A better, dynamical, description of correlations<sup>20</sup> between the  $3d$  electrons in chromium could not only change the shape of the 3D-ACAR spectra, but also the positions of the FS breaks. That a different treatment of  $e$ - $e$  correlations can lead to different spectra, through, e.g., a different distribution of the  $s$ ,  $p$ , and  $d$  characters of the electron wave function used in the calculation of  $\rho(\mathbf{p})$ , is illustrated in Fig. 4. In this figure, we have compared the original IPM curve, calculated with the LSD electron potential and wave functions, to two other  $\rho(\mathbf{p})$  curves, obtained, respectively, when artificially increasing and decreasing the  $d$  character of the electron wave function, while the sum of the characters remains equal to 1. Note that this artificial redistribution of the wave function characters leads to a substantial change of the slopes of the  $\rho(\mathbf{p})$  curves, in a similar manner to the  $e$ - $p$  correlation effects [compare curves of Fig. 4 with the WDA result in Fig. 2(a)]. Similar conclusions were reached by the authors of Ref. 7, who studied the influence of various electron potentials and charge distributions on the calculated  $e$ - $p$  momentum densities and their comparison with the experimental data.

In summary, we have studied possible causes of the observed differences between theory and experiment in the 3D-ACAR spectra of Cr. We note that the same discrepancy also seems to occur for V and W. The calculated electronic structures of Cr and V are very similar, leading to highly anisotropic electron momentum densities, with the FS breaks in

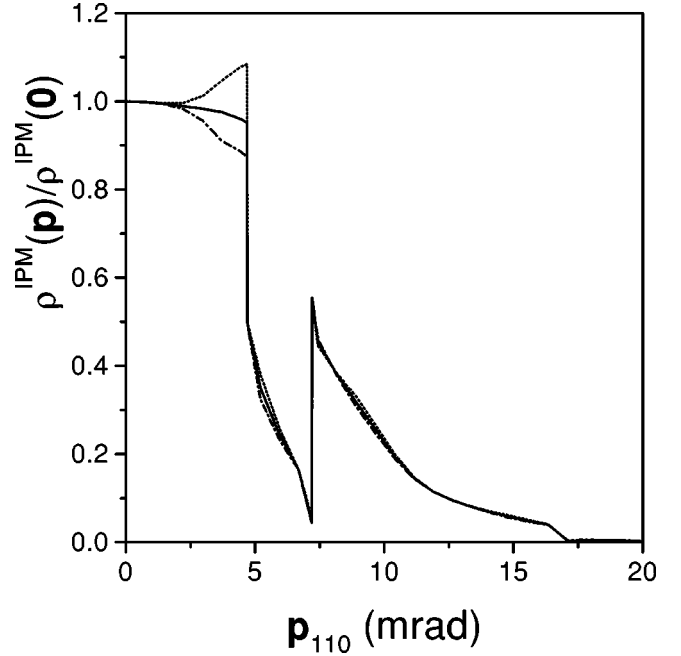


FIG. 4. Electron-positron momentum density for paramagnetic Cr along the [110] direction, calculated within IPM (solid line), in comparison with the curve obtained by increasing the  $d$ -electron character in the electron wave function by a factor of 1.1 (dotted line) and another curve obtained by reducing this character by a factor of 0.9 (dash-dotted line) relative to the original IPM result.

the [110] direction. By substantial increase of the FWHM of the resolution function, Matsumoto and Wakoh<sup>11</sup> were able to achieve reasonable agreement between the theoretical and experimental  $N$ -hole sizes for 2D projections of the  $e$ - $p$  momentum densities in V and Cr. However, our calculations convoluted with 3D Gaussians have not resulted in similar improvements, especially regarding the FS break in the [110] direction. This could indicate both inadequate description of  $e$ - $e$  correlations and inaccuracy of the reconstruction techniques. Perhaps, also the  $e$ - $p$  correlations should have been treated more accurately. It seems that the 3D-ACAR reconstruction techniques are able to describe the FS topology, but they are less successful in reproducing the full anisotropy of the EMD's, as predicted for these systems by the present day band theory. For Cr the 3D reconstructed results are found to be rather isotropic for all studied symmetry directions, and eliminating the observed discrepancy between theory and experiment will have to involve further studies and developments. Interestingly, in Compton scattering experiments one sees similar momentum densities that are more isotropic than the calculated ones.<sup>21</sup> In contrast to the electron-positron momentum densities, this occurs for all transition metals, and not only for the bcc ones. Electron-electron correlations have been shown to account only for part of the discrepancy<sup>22</sup> and final state effects have been equally important.<sup>23</sup>

We thank Professor M. Ashraf Alam and his group at Bristol University (UK) for providing us with the 3D recon-

structed electron-positron momentum densities for three different crystallographic directions in paramagnetic chromium. In particular, Dr. Stephen Dugdale is gratefully acknowledged for numerous discussions and help in understanding

details concerning the reconstructed data. We are also indebted to Dr. G. Kontrym-Sznajd, Dr. A. Jura, and Dr. A. Baranowski for helpful discussions, while Dr. H. Sormann and Dr. G. Banach are thanked for useful communications.

- <sup>1</sup>For review, see, e.g., S. Berko, in *Positron Solid State Physics*, edited by W. Brandt and A. Dupasquier (North-Holland, Amsterdam, 1983), p. 64; F. Sinclair, W. S. Farmer, and S. Berko, in *Positron Annihilation*, edited by P. G. Coleman, S. C. Sharma, and L. M. Diana (North-Holland, Amsterdam, 1982), p. 322; R. N. West, *Positron Studies of Condensed Matter* (Taylor and Francis, London, 1974); M.J. Puska and R.M. Nieminen, *Rev. Mod. Phys.* **66**, 841 (1994); R. M. Nieminen, in *Positron Spectroscopy of Solids*, edited by A. Dupasquier and A. P. Mills, Jr. (IOS Press, Amsterdam, 1995), p. 443.
- <sup>2</sup>A.M. Cormack, *J. Appl. Phys.* **35**, 2908 (1964); G. Kontrym-Sznajd, *Phys. Status Solidi A* **117**, 227 (1990); S.B. Dugdale, H.M. Fretwell, M.A. Alam, G. Kontrym-Sznajd, R.N. West, and S. Bandrzadeh, *Phys. Rev. Lett.* **79**, 941 (1997); M. Biasini, G. Kontrym-Sznajd, M.A. Monge, M. Gemmi, A. Czopnik, and A. Jura, *ibid.* **86**, 4616 (2001).
- <sup>3</sup>S. B. Dugdale (private communication); 3D reconstructed experimental spectra have been kindly provided by Professor M. A. Alam and his group at Bristol University (UK).
- <sup>4</sup>T. Kubota, H. Nakashima, H. Kondo, and S. Tanigawa, *Mater. Sci. Forum* **105-110**, 719 (1992); T. Kubota, H. Kondo, H. Nakashima, and S. Tanigawa, *Phys. Status Solidi B* **168**, 179 (1991).
- <sup>5</sup>L.M. Pecora, *J. Phys.: Condens. Matter* **1**, SA1 (1989); L.M. Pecora, A.C. Ehrlich, A.A. Manuel, A.K. Singh, and R.M. Singru, *Phys. Rev. B* **37**, 6772 (1988).
- <sup>6</sup>G. Kontrym-Sznajd (private communication).
- <sup>7</sup>H. Sormann and M. Šob, *Phys. Rev. B* **41**, 10 529 (1990); **64**, 045102 (2001).
- <sup>8</sup>A. Rubaszek, Z. Szotek, and W.M. Temmerman, *Phys. Rev. B* **58**, 11 285 (1998); **61**, 10 100 (2000); **63**, 165115 (2001).
- <sup>9</sup>S. B. Dugdale, Ph. D. thesis, University of Bristol, 1996; S.B. Dugdale, H.M. Fretwell, D.C.R. Hedley, M.A. Alam, T. Jarlborg, G. Santi, R.M. Singru, V. Sundarajam, and M.J. Cooper, *J. Phys.: Condens. Matter* **10**, 10 367 (1998) and references cited therein; H.M. Fretwell, S.B. Dugdale, R.J. Hughes, J. Brader, M.A. Alam, and A. Rodrigues-Gonzales, *ibid.* **10**, 10 375 (1998).
- <sup>10</sup>N. Shiotani, T. Okada, H. Skizawa, S. Wakoh, and Y. Kubo, *J. Phys. Soc. Jpn.* **43**, 1229 (1973); C. Bull, A. Alam, N. Shiotani, A. K.Singh, and R. M. Singru, in *Positron Annihilation*, edited by P. C. Jain, R. M. Singru, and K. P. Gopinathan (World Scientific, Singapore, 1985), p. 266; A.K. Singh, A.A. Manuel, and E. Walker, *Europhys. Lett.* **6**, 67 (1988); P. Genoud, Ph. D. thesis, Geneva University, 1990.
- <sup>11</sup>M. Matsumoto and S. Wakoh, *J. Phys. Soc. Jpn.* **55**, 3948 (1986).
- <sup>12</sup>E. Fawcett, *Rev. Mod. Phys.* **60**, 209 (1988); **66**, 25 (1994).
- <sup>13</sup>A. Rubaszek, Z. Szotek, and W.M. Temmerman, *Acta Phys. Pol. A* **99**, 473 (2001).
- <sup>14</sup>H. Sormann (private communication); H. Sormann, G. Kontrym-Sznajd, and R.N. West, *Mater. Sci. Forum* **363-365**, 609 (2001).
- <sup>15</sup>P. Hohenberg and W. Kohn, *Phys. Rev.* **136**, B364 (1964); W. Kohn and L.J. Sham, *ibid.* **140**, A133 (1965).
- <sup>16</sup>J.P. Perdew and A. Zunger, *Phys. Rev. B* **23**, 5048 (1981).
- <sup>17</sup>O.K. Andersen, *Phys. Rev. B* **12**, 3060 (1975); W.R.L. Lambrecht and O.K. Andersen, *ibid.* **34**, 2439 (1986).
- <sup>18</sup>G. Banach (private communication); using WIEN97 code, P. Blaha, K. Schwarz, and J. Luitz, computer code WIEN97 (Karlheinz Schwarz, Techn. Universität Wien, Austria, 1999).
- <sup>19</sup>C.K. Majumdar, *Phys. Rev.* **140**, A227 (1963).
- <sup>20</sup>A. Georges, G. Kotliar, W. Krauth, and M.J. Rozenberg, *Rev. Mod. Phys.* **68**, 13 (1996); I. Yang, S.Y. Savrasov, and G. Kotliar, *Phys. Rev. Lett.* **87**, 216405 (2001).
- <sup>21</sup>G.E.W. Bauer and J.R. Schneider, *Phys. Rev. B* **31**, 681 (1985).
- <sup>22</sup>C. Filippi and D.M. Ceperley, *Phys. Rev. B* **59**, 7907 (1999).
- <sup>23</sup>J.A. Soinenen, K. Hämäläinen, and S. Manninen, *Phys. Rev. B* **64**, 125116 (2001).